

Research Article

Comparison of Response Surface Methodology (RSM) and Artificial Neural Networks (ANN) in Optimisation of the Thermal Diffusivity of Mild Steel TIG Welding

Augustine Oghenekevwe Igbinke * 

Department of Production Engineering, University of Benin, Benin City, Nigeria

Abstract

This study compares the effectiveness of Response Surface Methodology (RSM) and Artificial Neural Networks (ANN) in optimizing the thermal diffusivity of mild steel Tungsten Inert Gas (TIG) welds. The analysis evaluates the predictive accuracy and optimization efficiency of both techniques, providing insights into their suitability for modeling thermal behavior in welding applications. The set of tools, including power hacksaw cutting and grinding machines, mechanical vice, emery (sand) paper and sander was used to prepare the mild steel coupons for welding. The produced coupons were evaluated for their Thermal Diffusivity. The two expert systems used to determine the effect of the interaction of welding current, welding voltage and gas flowrate on the Thermal Diffusivity were the Response Surface Methodology and Artificial Neural Network. The models were validated using the model summary values between the experimental results compared to RSM ($R^2 = 94.49\%$) and ANN ($R^2 = 97.83\%$) values. This shows that ANN is a better predictor as compared to RSM.

Keywords

Thermal Diffusivity, Mild Steel, TIG, Gas Flowrate, Current, Voltage

1. Introduction

Thermal diffusivity is a fundamental property that describes how efficiently a material conducts thermal energy in relation to its ability to store heat. It is mathematically defined as the ratio of thermal conductivity (k) to the product of density (ρ) and specific heat capacity (C_p), expressed as:

$$\alpha = k/\rho C_p$$

where α represents thermal diffusivity (m^2/s), k is thermal conductivity ($J/m \cdot K \cdot s$), ρ is density (kg/m^3), and C_p is specific heat capacity ($J/kg \cdot K$) [1]. Due to its role in heat trans-

fer, thermal diffusivity is sometimes referred to as "temperature conductivity."

In the context of flame spread over porous solids soaked in liquid fuel, variations in thermal diffusivity significantly influence combustion behavior. Research has shown that the intensity of combustion differs across materials with different thermal diffusivities [2, 3]. For instance, flames exhibit more vigorous combustion over steel beads compared to sand and zeolite, a phenomenon attributed to differences in thermal diffusivity. Steel beads possess a thermal diffusivity approximately ten times greater than sand beds and about

*Corresponding author: Igbinke@gmail.com (Augustine Oghenekevwe Igbinke)

Received: 17 February 2025; **Accepted:** 3 March 2025; **Published:** 28 March 2025



five times higher than zeolite beds.

This distinction highlights a critical aspect of flame dynamics: materials with higher thermal diffusivity exhibit faster thermal response times to temperature changes. Consequently, the rate of flame spread is notably affected, with higher diffusivity materials facilitating more rapid heat transfer, thereby influencing combustion efficiency and fire propagation behavior.

Thermal Diffusivity is a material property that determines how fast heat can be conducted through a material. In welding, the Thermal Diffusivity of the base metal can affect the quality of the weld joint. In a study [4], it was found that the Thermal Diffusivity of the base metal had a significant effect on the formation of solidification cracks in the weld joint. The study observed that materials with low Thermal Diffusivity were more susceptible to solidification cracks.

A discussion on the accuracy of the method of determining the Thermal Diffusivity of solids using the solution of the inverse heat conduction equation was presented in their paper. A new procedure for data measurement processing was proposed to improve the effectiveness of the method. Using the numerical model [5], an analysis of the sensitivity of the method of Thermal Diffusivity determination to changes in operational and environmental parameters of the test was carried out. Their results showed that the method was insensitive to the parameters of the thermal excitation impulse, the thickness of the tested sample, and this significantly influence the accuracy of the cooling convection. The work was completed with the formulation of general conclusions concerning the conditions for determining the Thermal Diffusivity of materials with the use of the described method.

Thermal Diffusivity, thermal phase lag, conductance, thermal resistivity, thermal conductivity and thermal diffusivity were determined for two pieces of brick a new made sample and an old one. Samples were then coated with cement and measurements were repeated [6]. Thermal Diffusivity of the samples were found to range from 6.8×10^{-7} PmP 2 PsP -1 P to 18×10^{-7} PmP 2 PsP -1 P, thermal phase lag ranged between 5.6 hP -1 P and 29 hP -1 P while conductance ranged from 1.2 WmP - P²KP -1 P to 1.7 WmP - P²KP -1 P thermal resistivity ranged between $0.83 \text{ m}^2 \text{ K.WP}^{-1}$ P and $0.58 \text{ m}^2 \text{ K.WP}^{-1}$ P thermal conductivity was found to range from 1.6 WmP^{-1} PKP -1 P to 2.02 WmP^{-1} PKP -1 P whereas Thermal Diffusivity was found to range from 12.28×10^{-7} P23TWsP 1/2P/mP 2 PK23T to 23×10^{-7} P23T WsP 1/2P/mP 2 PK23T. All results were compared with previous studies.

In [7], estimates of thermal diffusivity (κ , K) for hydrocarbon-bearing horizons in the Chad Basin, northeastern Nigeria, obtained from density log data, show close agreement with values derived from temperature-time measurements. The observed scatter in the first estimation is attributed to random fluctuations, while the underestimation in the latter is likely due to data quality limitations. The trend of thermal diffusivity across these horizons suggests a common source

for intrusive formations. While pressure-induced variations in thermal diffusivity are considered negligible, temperature-induced effects are found to be significant. Furthermore, the rapid cooling of intrusions is believed to impact hydrocarbon maturation, potentially influencing hydrocarbon exploration and discovery.

The Thermal Diffusivity of three food products, Pent land Dell potato, malt bread and wheat flour, was determined using a Thermal Diffusivity tube under transient heat transfer conditions by two different methods, the log method and the slope method, both based on the solutions of the Fourier equation [8]. Both methods gave similar results for potato, 1.30×10^{-7} and $1.44 \times 10^{-7} \text{ m}^2 \text{ s}^{-1}$, flour, 1.00×10^{-7} and $1.04 \times 10^{-7} \text{ m}^2 \text{ s}^{-1}$, but different results for bread, 1.17×10^{-7} and $2.56 \times 10^{-7} \text{ m}^2 \text{ s}^{-1}$. The values were compared with a prediction model and with previously documented values. The measured values for potato and flour were found to be close to those calculated by the prediction model. The value for bread, calculated by the log method, was also close to the predicted value, but its Thermal Diffusivity calculated by the slope method was close to literature values.

The thermal diffusivity of various steel types was measured in [9] using the laser flash method, which relies on precise specimen thickness for accuracy. Additionally, the thermal expansion of steel was recorded over a temperature range from room temperature to 1676 K. At high temperatures, a decrease in steel thickness was observed and quantified using quenched samples. By integrating these findings, reliable thermal diffusivity values were determined for different steel compositions.

2. Material and Methods

2.1. Sample Preparation

According to the Experimental Matrix presented in Table 1, twenty sets of experiment were performed and 5 specimens were used for each run. The plate sample was 60 mm long with a wall thickness of 10mm. The sample was cut longitudinally with a single-V joint preparation as shown in Figure 1.

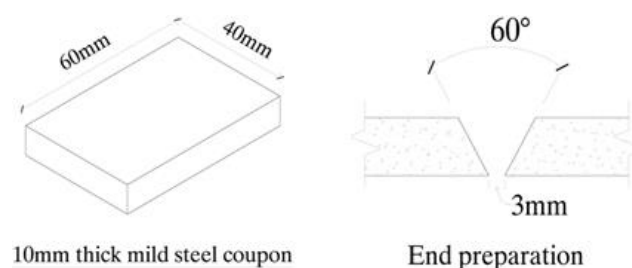


Figure 1. Weld specimen design.

The set of tools including power hacksaw cutting and

grinding machines, mechanical vice, emery (sand) paper and sander presented in Figure 2 was used to prepare the mild

steel coupons for welding.



Figure 2. Set of equipment for coupon preparation.

The set of tungsten inert gas welding equipment presented in figure 3 was used in welding the plates after the edges have been machined and bevelled.

welding process, thermal measurements, post weld tests and calculations.



Figure 3. Tungsten Inert Gas Welding Equipment.

Shield gas was used to protect the weld specimen from atmospheric interaction during the welding process. 100% pure Argon gas was used for this study. The weld samples were made from 10mm thickness of mild steel plate; the plate was cut to size with the power hacksaw. The edges grinded and surfaces polished with emery paper and the joints welded.

2.2. Data Collection

After grinding and polishing of the sample edges, welding work was carried out, and the responses were measured, recorded and presented in Table 1.

The Department of Welding and Fabrication Technology, Petroleum Training Institute laboratory was used for the TIG

Table 1. Design of Experiment (DoE) Matrix.

S/N	I Amp	E, Volt	GFR L/min
1	165.000	17.500	14.500
2	180.000	16.000	16.000
3	150.000	19.000	16.000
4	165.000	17.500	14.500
5	165.000	17.500	14.500
6	165.000	20.023	14.500
7	180.000	19.000	16.000
8	165.000	17.500	14.500
9	150.000	19.000	13.000
10	165.000	17.500	14.500
11	180.000	16.000	13.000
12	139.773	17.500	14.500
13	180.000	19.000	13.000
14	165.000	14.977	14.500
15	190.227	17.500	14.500
16	165.000	17.500	11.977
17	165.000	17.500	17.023
18	150.000	16.000	13.000
19	150.000	16.000	16.000
20	165.000	17.500	14.500

3. Result and Discussion

To analyse the data, the following expert models were employed:

1. Response surface methodology (RSM);
2. Artificial Neural Network (ANN).

3.1. Response Surface Methodology (RSM)

For analysis of design data, Design Expert Statistical Software, in order to obtain the effects, coefficients, standard deviations of coefficients, and other statistical parameters Version 13.0 was engaged for the fitted models. The behaviour of the system which was used to evaluate the relationship between the response variables (Y_T) and the independent variables (X_1, X_2 , and X_3) was explained using the empirical second-order polynomial equation [10].

$$Y = \beta_0 + \sum_{i=1}^q \beta_i x_i + \sum_{i=1}^q \beta_{ii} x_i^2 + \sum_{i=1, i < j=2}^{q-1} \sum_{j=2}^q \beta_{ij} x_i x_j + \varepsilon \quad (1)$$

where,

$X_1, X_2, X_3 \dots X_k$ = input variables;

$Y, \beta_0, \beta_i, \beta_{ii}$, and β_{ij} = the known parameters, and ε = the random error.

The Response Surface Model extends simple linear regression by incorporating second-order effects to account for non-linear relationships. It is a widely used optimization technique for identifying the optimal combination of variables to achieve a desired response. RSM is particularly valuable in modeling complex systems, as it helps analyze the interactions between multiple predictor variables and their corresponding responses [11].

3.2. Artificial Neural Network

The implementation of the Artificial Neural Network (ANN) in this study followed a structured approach, which is detailed in the following sections.

3.2.1. Experimental Design and Data Collection

A Central Composite Design (CCD) was employed to define the experimental conditions, specifying a total of 20 experimental runs. These experiments were conducted under varying welding current, welding voltage, and gas flowrate to generate the dataset required for the ANN model.

3.2.2. Data Normalization

To ensure consistency and improve model stability, the experimental results were normalized before further processing. The input and output variables were scaled within the range of 0.1 to 1.0 using a standard normalization equation [12], as presented in Equation 2. This step was crucial in preventing large variations in data from affecting the efficiency of the neural network training process.

$$x_i = \frac{x - x_{\min}}{x_{\max} - x_{\min}} + 0.1 \quad (2)$$

where,

x_i = the normalized value of input and output data

x_{\min} and x_{\max} are the minimum and maximum value of input and output data

x = the input and output data.

3.2.3. Data Partitioning

Following normalization, the dataset was randomly divided into three subsets to facilitate model training and evaluation:

1. Training set (70%) – Used for model learning and parameter adjustment.
2. Validation set (15%) – Used to monitor model performance and prevent overfitting.
3. Testing set (15%) – Used to assess the predictive accuracy of the final trained model.

By following this structured approach, the ANN was effectively trained and evaluated using the experimental data, ensuring reliable and accurate predictions.

The optimal equation which shows the individual effects and combine interactions of the selected input variables (current, voltage and gas flowrate) against the measured Thermal Diffusivity is presented based on the coded variables in equation 3.

$$1/\text{sqrt}(Y_T) = +0.5857 + 0.0501A + 0.0454B + 0.0358C + 0.0283AB - 0.0171AC - 0.0036BC + 0.0024A^2 + 0.0224B^2 + 0.0346C^2 \quad (3)$$

Where, Y_T = Thermal Diffusivity

ANN produced equation 4. with Table 2 as its model summary.

$$\text{EXP} = 0.1272 + 0.9428 \text{ RSM} \quad (4)$$

Table 2. Model Summary for RSM Thermal Diffusivity.

S	R-sq	R-sq(adj)
0.146883	94.49%	94.18%

Table 3. Experimental observed value RSM predicted vs ANN predicted result of Thermal Diffusivity responses.

S/N	Input parameters			Exp	RSM prediction	ANN
	Current	voltage	GFR	Responses Thermal Diffusivity	Thermal Diffusivity	Prediction Thermal Diffusivity
1	165.000	17.500	14.500	2.849	2.924	2.916
2	180.000	16.000	16.000	2.370	2.253	2.405
3	150.000	19.000	16.000	2.221	2.395	2.368
4	165.000	17.500	14.500	3.016	2.924	2.916
5	165.000	17.500	14.500	2.855	2.924	2.916
6	165.000	20.023	14.500	1.931	1.813	1.914
7	180.000	19.000	16.000	1.625	1.651	1.612
8	165.000	17.500	14.500	3.014	2.924	2.916
9	150.000	19.000	13.000	3.210	3.175	3.186
10	165.000	17.500	14.500	2.855	2.924	2.916
11	180.000	16.000	13.000	2.867	3.115	2.732
12	139.773	17.500	14.500	3.877	3.729	3.746
13	180.000	19.000	13.000	1.737	1.741	1.665
14	165.000	14.977	14.500	3.004	3.479	3.005
15	190.227	17.500	14.500	2.191	2.078	2.305
16	165.000	17.500	11.977	2.531	2.476	2.659
17	165.000	17.500	17.023	1.839	1.885	1.696
18	150.000	16.000	13.000	3.666	3.661	3.691
19	150.000	16.000	16.000	2.5161	2.605	2.599
20	165.000	17.500	14.500	2.905	2.924	2.916

Table 3 presents the comparison between the experimental value, RSM and the ANN predicted value for Thermal Diffusivity responses against the welding current, welding voltage and the gas flowrate.

The model summary values between the experimental results compared to RSM ($R^2 = 94.49\%$) and ANN ($R^2 = 97.83\%$) values. This shows that ANN is a better predictor as compared to RSM.

Figure 4 presents the time series plot showing the prediction accuracies of RSM and ANN to experimental for indi-

vidual run number.

A time series plot is a graphical representation of data points collected over time, allowing for the visualization of trends, patterns, or seasonal variations in the data. Figure 4 shows the prediction accuracy of the two expert systems used against the experimental for predicting Thermal Diffusivity response. By examining the plot, one can see, that even with the limited data set for training, validation and testing, ANN performance is also in close approximation with the experimental trend.

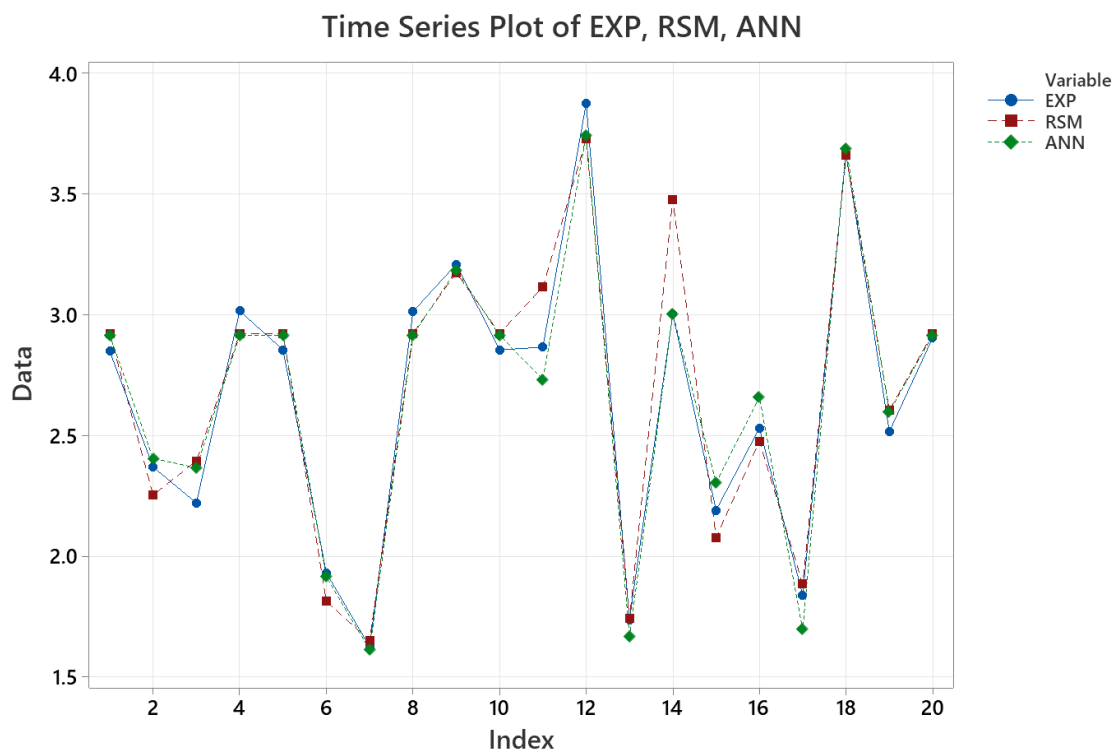


Figure 4. Time series plot showing the prediction accuracy of ANN and RSM in comparison to Experimental for Thermal Diffusivity responses.

4. Conclusion

1. Results obtained in this study showed that the interactive combination of current and voltage has a very significant influence on Thermal Diffusivity.
2. Increase in current and voltage increased the Thermal Diffusivity.
3. The optimum result from RSM indicated a desirability value of 91.5% at the gas flowrate of 13L/min.
4. The ANN results showed significant compliance and validation of the experimental and numerical results, with ANN having better prediction accuracy.

Abbreviations

ANN	Artificial Neural Network
CCD	Central Composite Design
DoE	Design of Experiment
EXP	Experiment
GFR	Gas Flowrate
RSM	Response Surface Methodology

Author Contributions

Augustine Oghenekevwe Igbinate is the sole author. The author read and approved the final manuscript.

Conflicts of Interest

The author declares no conflicts of interest.

References

- [1] Jafar Z, Behdad M, Hiroki I (2013) Combustion and flame spread on fuel-soaked porous solids progress in energy and combustion science volume 39, issue 4, august 2013, pages 320-339.
- [2] Chao CHY, Wang JH, Wenjun K (2004) Effects of fuel properties on the combustion behavior of different types of porous beds soaked with combustible liquid, International Journal of Heat and Mass Transfer 47 (2004) 5201–5210.
- [3] Chao, T. T., Ma, Y. Y., Li, M. W. (2019) Hydrocarbon Characteristics of Inter-Salt System in Qian 3 Member of Qianjiang Sag, Jiangnan Basin and Their Indication. Journal of Xi'an Shiyou University (Natural Science Edition), 34, 25-30.
- [4] Chen, H. M, Wang Q, Geng D. L, Wang H. P (2021). Specific heat, Thermal Diffusivity, and thermal conductivity of Ag–Si alloys within a wide temperature range of 293–823 K, Journal of Physics and Chemistry of Solids Volume 153, June 2021, 109997.
- [5] Adam Adamowicz (2022), determination of Thermal Diffusivity values based on the inverse problem of heat conduction – numerical analysis, acta mechanica et automatica, vol. 16 no. 4 (2022) 399.

- [6] PHuda M. Kamal, P PMarah Mohamed (2021) Determination of Thermal Conductivity, Thermal Diffusivity and Thermal Effusivity in Fired Clay Bricks, *International Journal of Innovative Science, Engineering & Technology*, Vol. 8 Issue 10, October 2021 ISSN (Online) 2348 – 7968.
- [7] Ali SK, musto- onuaha, orazulike d. m., (2004) Thermal Diffusivity estimates in the chad basin, N. E. nigeria-implications for petroleum exploration, *ASSET An International Journal Series B* (2004) 3(1): 155-171.
- [8] Magee TRA. And Bransburg T (1995) Measurement of Thermal Diffusivity of potato, malt bread and wheat flour *Journal of Food Engineering* Volume 25, Issue 2, 1995, Pages 223-232.
- [9] Tsuyoshi N, Hiroyuki S, Koichi T, Hiromichi O, Yoshio W, (2002) Measurement of Thermal Diffusivity of Steels at Elevated Temperature by a Laser Flash Method *ISIJ International* 42(5): 498-503.
- [10] Nuran, B. (2007) *The Response Surface Methodology*. Master of Science in Applied Mathematics and Computer Science, PhD Dissertation, Faculty of the Indiana University, South Bend.
- [11] Igbinake, A. O., Achebo, J. I., Obahiagbon, K. O. and Ozigagan, A.; (2023) application of expert methods to enhance the impact energy of v-butt weldment *Journal of Engineering for Development*, Vol. 15(1), March (2023) pp. 26-36.
- [12] Sinan, M. T; Beytullah, E and Asude, A (2011), Prediction of adsorption efficiency for the removal of Ni(II) ions by zeolite using artificial neural network (ANN) approach, *Fresenius Environmental Bulletin*, vol. 20(12), pp; 3158-3165.